Geospatial Modeling of Aeolian Dynamics in the Algerian Steppe from Zahrez Chergui to Hodna

Abdelmalek Rerboudj
Laboratory of Geomorphology and Geo-risks, Faculty of Earth Science, University of Sciences and Technology Houari Boumediene, Algeria
a.rerboudj@univ-batna2.dz (corresponding author)

Mohamed-Said Guettouche
Laboratory of Geomorphology and Geo-risks, Faculty of Earth Science, University of Sciences and Technology Houari Boumediene, Algeria
mguettouche@usthb.dz

Yann Callot
University of Lumiere Lyon 2, Archeorient, Maison de l'Orient et de la Mediterranee, France
yann.callot@univ-lyon2.fr

Received: 25 September 2024 | Revised: 23 October 2024 | Accepted: 31 October 2024

 DOI: https://doi.org/10.48084/etasr.9095

ABSTRACT

Assessing the hazards associated with aeolian geomorphological processes requires a fundamental understanding of their spatial distribution. These phenomena often have detrimental impacts on the environment, economy, and society. This problem is prevalent in the Algerian steppe, encompassing the Zahrez, Chergui, and Hodna regions. This study proposes a research method for developing more accurate and simpler indices to evaluate the extent and directionality of sand migration. Specifically, it examines surface characteristics, such as altitude, slope, and slope exposure. However, some tools used for spatial modeling of wind dynamics necessitate corrections to account for the effects of topography and surface features on wind, which for this study are implemented using spatial techniques. The results are incorporated into the model developed by Fryberger, which requires wind data and a Digital Surface Model (DSM) to estimate the factors included in this model. The findings indicate that the average potential quantity of sand movement is 64 t m^{-1} yr^{-1} over the entire study area, with 37.3% of the region experiencing severe deflation of 140 t m^{-1} yr^{-1}. This result can be utilized to enhance the understanding of the direction and magnitude of sand movement in any region.

Keywords-spatial modeling; aeolian dynamics; wind exposure index; wind amplification index; algerian steppe

I. INTRODUCTION

The spatial distribution of aeolian processes is critical in assessing the risks associated with this phenomenon. The consequences can have environmental and socioeconomic impacts, several of which are more severe in arid and semi-arid regions [1-3]. Wind erosion and sand displacement are problems in the Algerian steppe, which encompasses/constitutes the study area [4]. Topography influences sand movement patterns, affecting the spatial distribution of dunes, particularly in the area south of the Algiers Steppe at Hodna or Zahrez Chergui [5-8].

The Fryberger method has become the dominant and effective approach for quantifying aeolian geodynamics since its development [9]. While this formula is not foolproof, it remains widely utilized to evaluate wind patterns in vector units and estimate the potential for sand transport in these wind conditions [10, 11]. This method was based on the Lettau H. and Lettau K. equation, which primarily relied on aerological data [12]. The Fryberger method produces adequate results when other factors are conducive, such as the conditions observed at Cap Juby in Morocco [13, 14]. However, corrections for any additions or modifications, or the concurrent use of a complementary index, may be necessary in other circumstances.

Natural phenomena are heavily influenced by topographic features that impact climate, wind erosion, and sand displacement in various scales [15-18]. Obstacles, such as

rocks or vegetation of different sizes and textures, affect the shape and geometry of dunes [19]. A relationship between potential sand movement and dune slope has been developed on a local level [20], given by:

$$\frac{dQ}{dx} = \gamma\, C \tan\alpha \quad (1)$$

where, γ is the density of sands, C is the displacement rate, and α is positive in windward areas and negative in leeward areas [21]. A correction coefficient has been also developed in the form given by [22]:

$$q' = G * q \quad (2)$$

where, G is the coefficient of correction of slope effects on the quantity of sand transported, q represents the quantities of potential sand displacements on a plane, while q' denotes the quantities of potential sand displacements on the slope ± θ. To account for the effects of slope on the sand transport rate, G is calculated as:

$$G = \tan\alpha/(\cos\theta * (\tan\alpha + \tan\theta)) \quad (3)$$

where, α is the internal friction angle of the sediments and assumed to be 32°, and θ is the slope of the surface with positive and negative values depending on the exposure to the wind.

The wind amplification factor (A_z) represents the ratio of the average wind speed at height z (V_2) to the average speed in a flat area (V_1) [23, 24]. This factor ranges from 1.1 to 2 for small and medium-sized dunes [25, 26]. Additionally, on a dune in Silver Peak, Nevada accelerations are measured and range from 1.50 to 3.19 [27]. Sand deposition is strongly correlated with the obstacle height-to-width ratio, as observed and tested in a wind tunnel [26, 28]. The formation and thickness of dunes are determined by the obstacle's characteristics, such as height, width, length, and slope, as well as the direction of sand movement. For example, the shape of a dune can be expressed as $h = \left(\frac{W}{2}\right) * \tan\theta$ [29]. It is shown that topography can affect the threshold velocity of sand particles [30, 31]. Furthermore, using Bagnold's equation, the sand transport rate is more related to terrain slope [20, 32]. Therefore, two correction coefficients were created: one to correct the threshold velocity of movement and another to correct sand transport. Wind tunnel experiments were conducted to test the effect of slope on wind, saltation threshold, and sand transport across a granulometric range of 124-544 µm [33, 34].

On a regional scale, it was determined that the rocky massif had a significant impact on the formation of the Fachi-Bilma erg [28]. Wind speed changes are strongly correlated with the characteristics of the obstacle. The position of ergs in relation to large reliefs can influence the shape of erg dunes, and the aerodynamics of this obstacle's position facing the wind flow [35, 36]. Additionally, ergs are consistently found in topographic depressions, either on the windward or leeward side [37-39]. These ergs are frequently affected by wind action or hydro-aeolian activity. A correlation was discovered between the surface roughness index, topography, and vegetation in coastal areas [40]. The amount of sand deposited is largely determined by the obstacle's distance and height [26, 41-43].

This study seeks to develop a model for quantifying aeolian geodynamics, enabling estimates of sand flux displacement direction. The proposed approach involves creating a climate index that utilizes spatial techniques to account for the influence of topography on winds, incorporating the amplification coefficient. The wind power was assessed by analyzing topographic features derived from the DSM covering the study area, and this index was subsequently incorporated into the Fryberger model.

II. MATERIALS AND METHODS

A. Study Area

The study area expands over 9694.8 km^2, situated between the Zahrez Chergui basin and the southern and southwestern Hodna basin, bounded by latitudes 34.82 ° and 35.47 ° north and longitudes 3.01 ° and 4.80 ° east, and is present in Figure 1. This region exhibits a prominent sand ridge that stretches approximately 161 km, with a width ranging from 3 to 5 km and a total area of around 644 km². The surface of this feature is subject to fluctuations driven by climatic conditions. Scholarly research suggests that dunes can form in a belt-like pattern due to various factors, such as climate and topography, resulting in a wind corridor pattern across the landscape [44, 45].

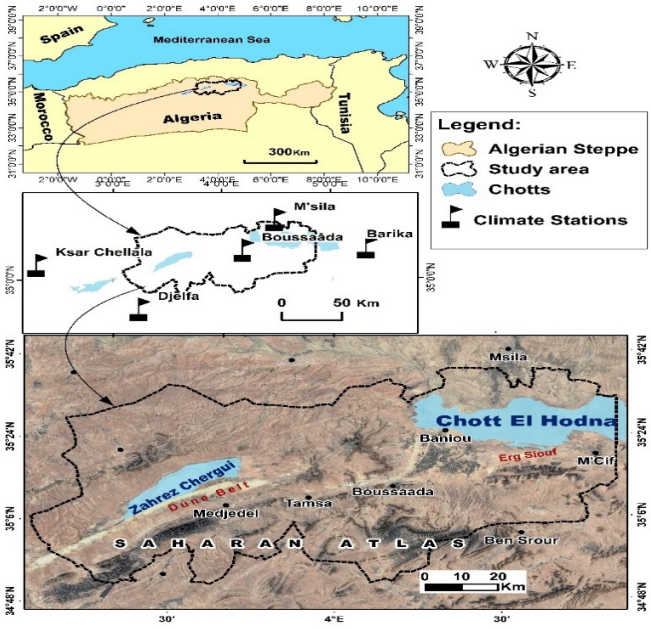

Fig. 1. Location of the study area.

The study region exhibits a semi-arid climate in the mountainous areas and an arid climate in the vicinity of Chott Hodna. The winter months are characterized by cold temperatures, with the average monthly temperature range fluctuating between 1 °C and 5 °C, while the summer season is marked by dry conditions and average temperatures between 34 °C and 40 °C. From 1984 to 2015, the annual mean

temperature varied from 15 °C at Zahrez Chergui to 20 °C at Hodna. The annual relative humidity was recorded as 51% in Boussaâda and 58% in Djelfa. During the winter and spring seasons, the predominant wind directions were from the north and northwest, with an average monthly wind speed from 3.4 to 4.7 m/s. Conversely, the summer and autumn periods were dominated by winds from the south and southwest, with average monthly wind speeds ranging from 3.4 to 5 m/s.

B. Data Collection

The study obtained wind data from Algeria's National Office of Meteorology (ONM) and the NOAA website [46]. The dataset spans 20 years, from 1995 to 2015, for four stations including Boussaâda, M'sila, Djelfa, and Ksar Chellala. The station of Barika provided data for 4 years. The wind recordings are taken at intervals of 1, 3, or 8 hours depending on the station. The quality of the data was evaluated by comparing the number of gaps to the total number of measurements. For example, the Boussaâda station had 0.96% and 0.99% gaps in wind speed and direction, respectively. Additionally, the study utilized USGS Landsat OLI and Google Earth Pro imagery, as well as the ALOS Global DSM [47, 48]. Field data were collected through 1 kg mobile sand samples from dune crests using a Garmin 62s GPS, distributed along the sand transport direction. The sand bulk density along the dune belt between the Zahrez Chergui and Hodna basins was estimated at the Lumière Lyon 2 University's OMEA platform laboratory.

C. Methodology

The data enabled the implementation of multiple treatments using the steps outlined in the flowchart depicted in Figure 2.

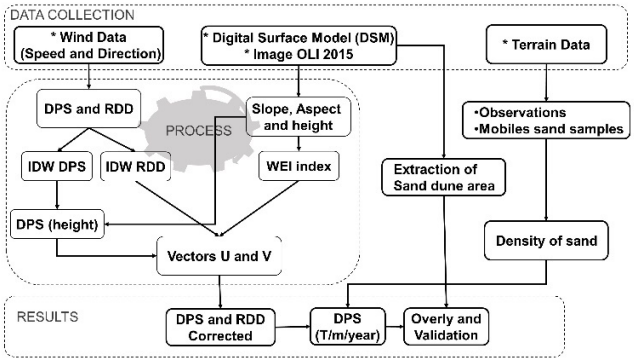

Fig. 2. Flowchart of the adopted methodology.

1) Calculation of the Wind Regime

The method is primarily based on calculating a set of parameters, modified by (4) and (5), specifically the Potential Sand Displacement (DPS) and the Resultant Drift Direction (RDD) [2, 3, 9, 12, 49, 50].

$$DPS = \sum_{i=1}^{16} U^2 \, (U - U_t)t \quad (4)$$

$$\text{RDD} = \arctan\left(\sum_{i=1}^{16}(\text{VU})\sin(\text{Dir}_i) \,/\, \sum_{i=1}^{16}(\text{VU})\cos(\text{Dir}_i)\right) \quad (5)$$

where U is wind velocity, and U_t is the impact threshold velocity, which for this paper is considered approximately 6 m/s [3, 51, 52]. Moreover, t is the time during which U receives higher values than Ut, expressed as a percentage, Dir_i is the angle of wind direction and is measured clockwise from the north, which has the 0 ° value, and VU in/is the drift potential in each wind direction class.

2) Topographic Correction of DPS and RDD Parameters

To begin with, Wind Exposure Index (WEI) is calculated as [53]:

$$WEI = \cos\theta = \cos\mu * \sin\beta + \sin\mu * \cos\beta * \cos(\delta - \gamma) \quad (6)$$

where μ is the slope of the terrain, γ is the slope exposure, δ is the azimuth of winds and in this study is considered equal to RDD, and β is the horizon angle in the wind direction equal to 0 [53]. The WEI values spanned the range from -1 to +1. The slopes facing the wind exhibited positive values, while those on the leeward side exhibited negative values.

Furthermore, the wind amplification for topography is calculated as:

$$\frac{U_{z1}}{U_{z2}} = \left(\frac{z1}{z2}\right)^{\alpha} \quad (7)$$

where U_{Z1} is the wind speed at height $z1$, U_{Z2} is the wind speed at reference height $z2$ equal to 10 m, and α is an exponent equal to 1/7 [54]. This parameter represents the topographic roughness, which influences wind profiles and flows over flat terrain [55]. Its value commonly falls within the range from 0.1 to 0.3, with 1/7 denoting the average condition [56-58].

Furthermore, the interpolation and correction of topographic effects on the wind regime follows a number of steps depicted below. Assuming that $Q = DPS$ and $Q_0 = DPS_0$ are on the same flat zone, the DPS is equal to the cubic value of the wind speed, $Q \propto V^3$ [20]. If the value of the speed (V) is replaced using (8), the following ratio is received:

$$\frac{Q}{Q_0} = \frac{V^3}{V_0^3} = \frac{V}{V_0} = \left(\frac{Z}{Z_0}\right)^{\alpha} \quad (8)$$

Thus, the correction of the topographic effects of DPS is calculated using:

$$DPS = DPS_0 * \left(\frac{Z}{Z_0}\right)^{\alpha} \quad (9)$$

Additionally, the DPS vector is calculated by (10), its magnitude by (11), and its direction by (12) [9, 59]:

$$\overrightarrow{DPS} = \begin{pmatrix} \text{U} = -\left(\text{U}_{z2} * \left(\frac{\text{Z1}}{\text{Z2}}\right)^{1/7}\right) * (\sin(\text{Dir}) + \sin(\theta)) \\ \text{V} = -\left(\text{U}_{z2} * \left(\frac{\text{Z1}}{\text{Z2}}\right)^{1/7}\right) * (\cos(\text{Dir}) + \cos(\theta)) \end{pmatrix} \quad (10)$$

$$\text{DPS} = \sqrt{\text{U}^2 + \text{V}^2} \quad (11)$$

$$\text{RDD (°N)} = \text{atan}\left(\frac{\text{V}}{\text{U}}\right) * 57.296 \mp 180 \quad (12)$$

The proposed method quantifies DPS and the resulting RDD across the study area, including the dune crest. This information can be leveraged to enhance the understanding of the wind patterns and the scale of sand displacement.

This approach generally comprises three stages, illustrated in Figure 3. Firstly, the data acquisition phase, which incorporates wind data and calculations of wind regime parameters, as well as the DSM utilized to determine topographical factors, such as slope, elevation, and slope orientation. This is then followed by the modeling phase, which primarily focuses on wind exposure indices, wind amplification indices, and vectors of wind regime parameters, and finally the results phase, which concentrates on wind dynamics. These findings provide insights into the magnitude and direction of aeolian sand transport.

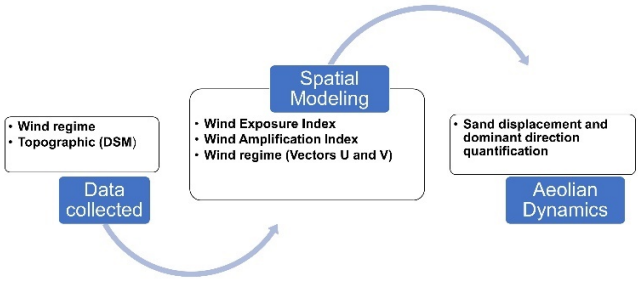

Fig. 3. Flowchart of the general methodology of topographic correction of DPS and RDD parameters.

III. RESULTS

A. Wind Regime

Table I summarizes the application of the Fryberger's model to the study stations and the sand density along the dune cord.

TABLE I. DPS CONVERSION TO VOLUME AND MASS PER STATION

Station	Boussaâda	M'sila	Barika	Djelfa	Ksar Chellala
DPS (*VU*)	823	685	832	758	625
RDP (*VU*)	538	328	124	288	456
CT	0.65	0.48	0.15	0.38	0.73
RDD (°N)	299.0	301.2	17.9	270.4	276.1
W (%)	19.7	24.2	25.9	24.8	21.0
Potential erosion ($m^3\ m^{-1}\ yr^{-1}$)	57	47.4	57.6	52.5	43.3
Density of sand ($kg\ m^{-3}$)[a]	1717	1717	1717	1769	1769
Potential erosion ($t\ m^{-1}\ yr^{-1}$)[b]	97.9	81.4	98.9	92.9	76.6

a. Sample. Density of sand was estimated at the OMEA laboratory of Lumière-Lyon2 University.

b. These masses present only potential and punctual quantities.

The DPS values exceed 400 *VU* across the study area, with a maximum observed in the center and eastern regions. The dominant winds originate from the west and north-northwest, except at the Barika station, where they are from the northeast. The directional variability coefficient (CT) is unimodal, except at Barika which is multimodal. The percentage of effective winds ranges from 19.7% at Boussaâda to 25.9% at Barika. The sand volumetric mass is 1717 kg m^{-3} at the Hodna stations and 1769 kg m^{-3} at Zahrez Chergui. To convert vectors to volumes, a mean volumetric mass of 1,743 t m^{-3} was used.

B. Interpolation and Correction of Topographical Effects on the Wind Regime

The sand movement parameters were interpolated using an Inverse Distance Weighting (IDW) method applied to the DPS and RDD datasets at a 30-meter spatial resolution. The DPS values ranged from 560 to 811 *VU*, with the highest values concentrated from the central to eastern portions of the study area. The resulting RDD directions spanned from west-southwest to west-northwest, specifically from 255 °N to 298 °N.

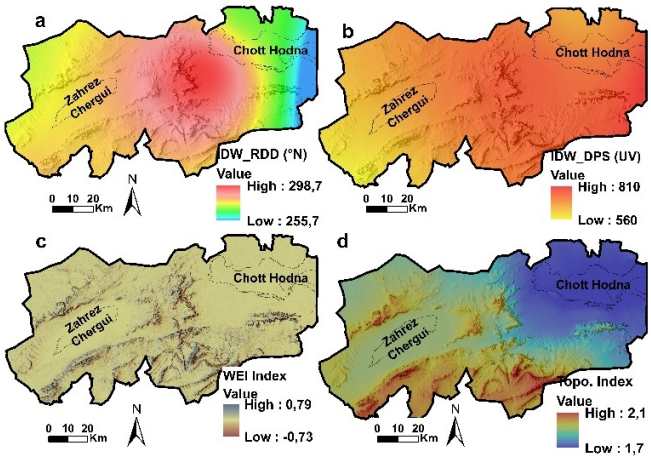

Fig. 4. Parameters of spatial modeling (a) IDW for RDD, (b) IDW for DPS, (c) WEI, and (d) is a topographic index.

The effects of elevation on DPS are adjusted using an amplification coefficient that varies from 1.7 to 2.1. The lowest values were noted in the vicinity of Chott Hodna, whereas the highest values were detected in the mountainous regions. The WEI was calculated and ranges from +0.79 in upwind areas to -0.73 in downwind areas [53].

C. Sand Displacement and Dominant Direction Quantification

The quantification of DPS reveals distinct wind energy patterns across the study region, as depicted in Table II and Figure 5. Table II indicates that 40% of the area experiences low wind energy, lower than 200 *VU*, with an estimated DPS below 24.1 t m^{-1} yr^{-1}. This low-energy zone encompasses the central and southern portions of the cordial dune belt at Zahrez Chergui, the western section of Erg Siouf, and the downwind areas. Conversely, 23% of the region is subjected to moderate wind energy between 200 *VU* and 400 *VU*, with a DPS ranging from 24.2 to 48.2 t m^{-1} yr^{-1}. This moderately exposed zone surrounds the low-energy area, located northeast of Zahrez Chergui and Erg Siouf. Furthermore, 37% of the study area is characterized by strong wind energy above 400 *VU*, with a DPS exceeding 48.3 t m^{-1} yr^{-1}. This high-energy class is situated in the central part of the study area, between Djebel Zemra, Temsa, Boussaâda, and Baniou, as well as to the east of M'cif, where the highest values are observed. The average DPS across the entire study area is 64 t m^{-1} yr^{-1}.

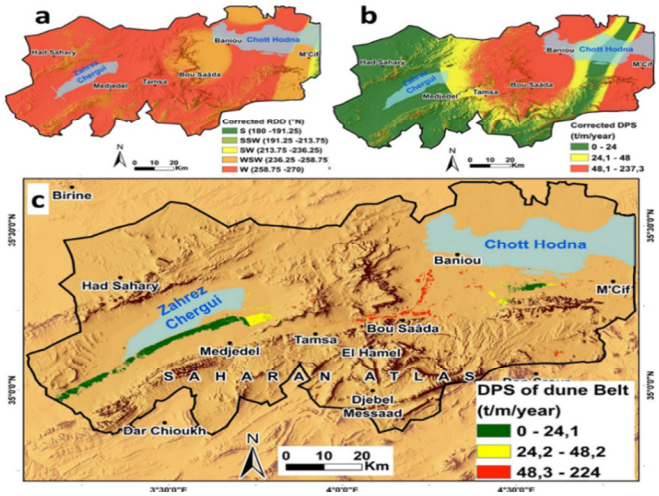

Fig. 5. (a) Corrected RDD, (b) Corrected DPS, and (c) DPS values on the Zahrez Chergui-Hodna dune belt.

TABLE II. SPATIAL DISTRIBUTION BY MASS DPS CLASSES AT ZAHREZ CHERGUI-HODNA (1995-2015)

DPS classes ($t\ m^{-1}\ yr^{-1}$)	Area	
	Km2	%
0 - 24	3868.4	39.9
24.1 - 48	2207.5	22.8
48.1 - 237.3	3618.9	37.3
Total	9694.8	100

IV. DISCUSSION

The point-based results are initially interpreted, followed by the interpolated findings deploying the IDW approach. In Boussaâda, with a total transport capacity of 823 *VU*, the potential movable sand volume is 56.9 m3 m^{-1} yr^{-1}, amounting to a mass of 97.7 t m^{-1} yr^{-1}. The observations are analogous to those from Barika, yet some reservations exist regarding the data from this station. Djelfa exhibits a slightly lower quantity compared to the previous locations, but it remains significant. Lacking in situ measurements, the reliability of these results cannot be assured. Nonetheless, they can be juxtaposed with findings from other studies. The proposed DPS spatial model aims to quantify DPS and their RDD using the factors depicted in Figure 3. According to the DPS interpolation map, areas with considerable sand accumulations correspond to regions with low or moderate wind energy. The amplification coefficient ranged from 1.7 to 2.1, which are comparable to the values of 1.1 to 2, and the 1.5 and 3.19 reported in several studies [25-27].

The areas with the lowest potential for sand displacement, i.e. less than 24.1 t m^{-1} yr^{-1}, due to low wind energy (less than 200 *VU*), are situated in the leeward regions. Zones with high wind energy, greater than 400 *VU*, and a high potential for sand displacement, greater than 48.3 t m^{-1} yr^{-1}, are found in wind-deflation zones. Furthermore, there is a zone with average wind energy, between 200-400 *VU*, that connects these two zones, characterized by an average DPS of 24.1 to 48.3 t m^{-1} yr^{-1}, such as the central area of Zahrez Chergui's dune belt and Erg Siouf in Hodna. Additionally, the region between Temsa, Boussaâda, and Baniou is known for its high wind energy. Large dune accumulations are absent, except for those trapped by topographical features, such as Djebel Kanfoude, as illustrated in Figure 6. The sand displacement is primarily from the west, which aligns with the directions reported by previous studies [8, 60].

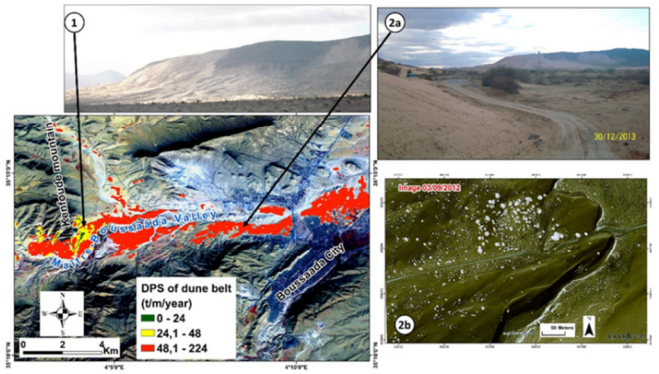

Fig. 6. Quantification of sand dynamics and silting risk between Kanfoude Mountain and Maiter Valley.

The analysis of the findings is based on previous studies [61]. For wind speeds exceeding 8 m/s, the 10-year average sand transport rates were determined to be 4.5 t m^{-1} yr^{-1} in Khiva, Uzbekistan, 38.7 t m^{-1} yr^{-1} in Kazandzhik, and 63.9 t m^{-1} yr^{-1} in Nebit-Dag, Western Turkmenistan. The latter result aligns with the present study's findings, which indicate a weighted average of 64 t m^{-1} yr^{-1} for the entire study area. In the Tarfaya region, a total displacement capacity of 1864 *VU* was previously estimated, with a volume of 120 m^3 m^{-1} yr^{-1}, but the actual displacement was found to be 160 m^3 m^{-1} yr^{-1}, equivalent to 200 t m^{-1} yr^{-1} [14]. This accounts for around 1/3, or more than 3 t m^{-1} yr^{-1}, which is consistent with the proposed methodology. The impact of vegetation on sand displacement was not considered in this study.

According to similar studies, in regions with moderate wind energy, the amount of sand transported is approximately 20 to 30 t m^{-1} yr^{-1} [51]. In the present study, the average quantity for this class is 36 t m^{-1} yr^{-1}, exceeding the class's maximum threshold by over 6 t m^{-1} yr^{-1}. The topographic characteristics of the study area, particularly elevation, slope, and slope exposure, significantly influence these results. Sand deposition is more prominent in downwind areas or as wind plating, while strong sand displacement occurs in regions which are the most exposed to winds. These values indicate satisfactory outcomes that accurately reflect the ground reality. The accuracy of this work could be improved by increasing the density and distribution of weather stations, as well as enhancing the spatial resolution of the DSM for better surface roughness estimation. Despite these limitations, the study remains valuable as it provides a simple and efficient approach to determine wind-driven sand movement.

V. CONCLUSION

This study presents a systematic and rigorous approach to modeling the sand movement dynamics on the southern steppe of Algiers. It provides a tool for pinpointing, strategizing, and

protecting areas susceptible to wind-driven processes, as well as informing future land use planning efforts. The goal of this approach is to develop more precise and user-friendly metrics for evaluating the potential magnitude and trajectories of sand mobilization driven by wind forces.

The result of applying this method shows that Hodna is more exposed to wind deflation phenomena, with a sand displacement rate exceeding 48.3 t/m/year. Furthermore, the medium and low rates are found in downwind areas. Over the entire study area, a weighted average Potential Sand Displacement (DPS) of 64 t/m/year from the west direction was estimated. These results are very much in line with field reality and with previous work indicating that this model gives very satisfactory results [13, 61].

This approach offers a research tool for generating more precise and user-friendly indices to assess the potential volume and direction of aeolian sand migration. It provides a valuable asset for identifying, forecasting, and safeguarding areas susceptible to aeolian dynamics, as well as for planning future land-use initiatives. Currently, there is an ongoing advancement in the development of a more accurate approach that integrates space-based remote sensing and machine learning technologies.

ACKNOWLEDGMENT

The authors express their gratitude to Mr. Jérôme Lejit and the staff of the laboratory of the platform Omea at University Lyon 2, as well as Mme. Vila Emmanuelle, Director of the Archéorient Laboratory at University Lyon 2. The authors also acknowledge the organizations NOAA, USGS Service, Jaxa-EORC Advanced Land Observing Satellite, and the National Office Meteorology of Algeria.

REFERENCES

[1] R. Khalil, M. S. Khan, Y. Hasan, N. Nacer, and S. Khan, "Supervised NDVI Composite Thresholding for Arid Region Vegetation Mapping," *Engineering, Technology & Applied Science Research*, vol. 14, no. 3, pp. 14420–14427, Jun. 2024, https://doi.org/10.48084/etasr.7202.

[2] M. R. Rahdari and A. Rodríguez-Seijo, "Monitoring Sand Drift Potential and Sand Dune Mobility over the Last Three Decades (Khartouran Erg, Sabzevar, NE Iran)," *Sustainability*, vol. 13, no. 16, Aug. 2021, Art. no. 9050, https://doi.org/10.3390/su13169050.

[3] B. Said, Youb Okkacha, B. Khaouani, D. Berrabah, and W. Djoudi, "Assessing Aeolian Sand Potential in Ain Sefra Region - Southwestern of Algeria," *Technium Social Sciences Journal*, vol. 30, pp. 710–726, Jun. 2022.

[4] H. N. L. Houérou, *Bioclimatologie et biogeographic des steppes arides du nord de l'Afrique - Diversite biologique, developpement durable et desertisation*. Montpellier, France: Centre International de Hautes Etudes Agronomiques Méditerranéennes), 1995.

[5] M. Benazzouz, "Étude des interactions relief-migrations éoliennes de sable dans la région de M'Doukal (Algérie)," *Méditerranée*, vol. 80, no. 3, pp. 51–54, 1994, https://doi.org/10.3406/medit.1994.2858.

[6] L. Boureboune and M. T. Benazzouz, "Aeolian Morphogenesis And Strategy Of Fight Against Desertification In Algeria (Hodna And Zibans Basin)," in *Desertification and Risk Analysis Using High and Medium Resolution Satellite Data*, Dordrecht, Netherlands, 2009, pp. 91–103, https://doi.org/10.1007/978-1-4020-8937-4_8.

[7] J. L. Ballais, A. Marre, and P. Rognon, "Périodes arides du Quaternaire récent et déplacement des sables éoliens dans les Zibans (Algérie," *Revue de géologie dynamique et de géographie physique*, vol. 21, no. 2, pp. 97–108, 1979.

[8] J. L. Ballais, "Recherches géomorphologiques dans les Aurès (Algérie)," PhD dissertation, Université de Paris 1, Paris, France, 1981.

[9] S. G. Fryberger and G. Dean, "Dune forms wind regime," in *A Study of Global Sand Seas*, vol. 1052, Washington, MD, USA: U.S. Government Printing Office, 1979, pp. 137–170.

[10] J. E. Bullard, "A note on the use of the 'Fryberger method' for evaluating potential sand transport by wind," *Journal of Sedimentary Research*, vol. 67, no. 3, pp. 499–501, May 1997, https://doi.org/10.1306/D42685A9-2B26-11D7-8648000102C1865D.

[11] K. I. Pearce and I. J. Walker, "Frequency and magnitude biases in the 'Fryberger' model, with implications for characterizing geomorphically effective winds," *Geomorphology*, vol. 68, no. 1–2, pp. 39–55, May 2005, https://doi.org/10.1016/j.geomorph.2004.09.030.

[12] K. Lettau, "Experimental and micrometeorological field studies of dune migration," University of Wisconsin-Madison, Institute for Environmental Studies, Madison, WI, USA, IES Report 101, 1978.

[13] Y. Callot and T. Oulehri, "Géodynamique des sables éoliens dans le Nord-Ouest saharien : relations entre aérologie et géomorphologie," *Geodinamica Acta*, vol. 9, no. 1, pp. 1–12, Mar. 1995, https://doi.org/10.1080/09853111.1996.11417259.

[14] T. Oulehri, "Etude géodynamique des migrations de sables éoliens dans la Province de Laayoune (Nord du Sahara marocain)," PhD dissertation, Université de Paris 6, Paris, France, 1992.

[15] J. Böhner and O. Antonić, "Chapter 8 Land-Surface Parameters Specific to Topo-Climatology," in *Developments in Soil Science*, vol. 33, T. Hengl and H. I. Reuter, Eds. Elsevier Ltd, 2009, pp. 195–226.

[16] J. P. Wilson and J. C. Gallant, *Terrain Analysis: Principles and Applications*. New York, USA: John Wiley & Son, Inc., 2000.

[17] J. P. Wilson, *Environmental applications of digital terrain modeling*. West Sussex, UK: John Wiley & Sons Ltd, 2018.

[18] J. Dujardin and M. Lehning, "Wind-Topo: Downscaling near-surface wind fields to high-resolution topography in highly complex terrain with deep learning," *Quarterly Journal of the Royal Meteorological Society*, vol. 148, no. 744, pp. 1368–1388, 2022, https://doi.org/10.1002/qj.4265.

[19] R. U. Cooke, A. Warren, and A. S. Goudie, *Desert Geomorphology*. Frome, UK: CRC Press, 1993.

[20] R. A. Bagnold, *The Physics of Blown Sand and Desert Dunes*. New York, USA: Dover Publications Inc., 1974.

[21] L. C. van Rijn and G. Strypsteen, "A fully predictive model for aeolian sand transport," *Coastal Engineering*, vol. 156, Mar. 2020, Art. no. 103600, https://doi.org/10.1016/j.coastaleng.2019.103600.

[22] D. J. Sherman, D. W. T. Jackson, S. L. Namikas, and J. Wang, "Wind-blown sand on beaches: an evaluation of models," *Geomorphology*, vol. 22, no. 2, pp. 113–133, Mar. 1998, https://doi.org/10.1016/S0169-555X(97)00062-7.

[23] J. J. Laity, *Deserts and desert environments*. West Sussex, UK: John Wiley & Sons Ltd, 2008.

[24] A. J. Bowen and D. Lindley, "A wind-tunnel investigation of the wind speed and turbulence characteristics close to the ground over various escarpment shapes," *Boundary-Layer Meteorology*, vol. 12, no. 3, pp. 259–271, Oct. 1977, https://doi.org/10.1007/BF00121466.

[25] N. Lancaster, "Variations in wind velocity and sand transport on the windward flanks of desert sand dunes," *Sedimentology*, vol. 32, no. 4, pp. 581–593, 1985, https://doi.org/10.1111/j.1365-3091.1985.tb00472.x.

[26] H. Tsoar, "Wind Tunnel Modeling of Echo and Climbing Dunes," in *Developments in Sedimentology*, vol. 38, M. E. Brookfield and T. S. Ahlbrandt, Eds. Elsevier, 1983, pp. 247–259.

[27] C. M. Neuman, N. Lancaster, and W. G. Nickling, "Relations between dune morphology, air flow, and sediment flux on reversing dunes, Silver Peak, Nevada," *Sedimentology*, vol. 44, no. 6, pp. 1103–1111, Dec. 1997, https://doi.org/10.1046/j.1365-3091.1997.d01-61.x.

[28] M. Mainguet and Y. Callot, in *L'Erg de Fachi-Bilma (Tchad-Niger). Contribution à la connaissance de la dynamique des ergs et des dunes des zones arides chaudes*, vol. 18, Paris, France: Éditions du Centre national de la recherche scientique, 1978, pp. 1–184.

[29] P. A. Hesp, "The formation of shadow dunes," *Journal of Sedimentary Petrology*, vol. 51, no. 1, pp. 101–111, Mar. 1981, https://doi.org/10.1306/212F7C1B-2B24-11D7-8648000102C1865D.

[30] A. D. HOWARD, "Effect of slope on the threshold of motion and its application to orientation of wind ripples," *GSA Bulletin*, vol. 88, no. 6, pp. 853–856, Jun. 1977, https://doi.org/10.1130/0016-7606(1977)88<853:EOSOTT>2.0.CO;2.

[31] A. D. Howard, J. B. Morton, M. Gad-El-Hak, and D. B. Pierce, "Sand transport model of barchan dune equilibrium," *Sedimentology*, vol. 25, no. 3, pp. 307–338, Jun. 1978, https://doi.org/10.1111/j.1365-3091.1978.tb00316.x.

[32] J. Hardisty and R. J. S. Whitehouse, "Effect of bedslope on desert sand transport," *Nature*, vol. 334, no. 302, Jul. 1988, https://doi.org/10.1038/334302b0.

[33] J. D. Iversen and K. R. Rasmussen, "The effect of surface slope on saltation threshold," *Sedimentology*, vol. 41, no. 4, pp. 721–728, Aug. 1994, https://doi.org/10.1111/j.1365-3091.1994.tb01419.x.

[34] J. D. Iversen and K. R. Rasmussen, "The effect of wind speed and bed slope on sand transport," *Sedimentology*, vol. 46, no. 4, pp. 723–731, Aug. 1999, https://doi.org/10.1046/j.1365-3091.1999.00245.x.

[35] M. Mainguet, "The influence of trade winds, local air-masses and topographic obstacles on the aeolian movement of sand particles and the origin and distribution of dunes and ergs in the Sahara and Australia," *Geoforum*, vol. 9, no. 1, pp. 17–28, Jan. 1978, https://doi.org/10.1016/0016-7185(78)90021-0.

[36] M. Mainguet, M. C. Chemin, and J. M. Borde, "Etude du rôle des obstacles topographiques dans la circulation éolienne d'après les images satellites et les photographies aériennes, de l'échelle continentale à celle de la butte-témoin [article]," *Méditerranée Télédéctection III*, vol. 54, pp. 11–19, 1985, https://doi.org/10.3406/medit.1985.2299.

[37] I. Livingstone and A. Warren, *Aeolian geomorphology: an introduction*. Harlow, UK: Longman, 1996.

[38] P. Kenneth and T. Haim, *Aeolian Sand and Sand Dunes*. Leipzig, Germany: Springer-Verlag Berlin Heidelberg, 2009.

[39] I. G. Wilson, "Ergs," *Sedimentary Geology*, vol. 10, no. 2, pp. 77–106, Oct. 1973, https://doi.org/10.1016/0037-0738(73)90001-8.

[40] N. Levin, E. Ben-Dor, G. J. Kidron, and Y. Yaakov, "Estimation of surface roughness (z0) over a stabilizing coastal dune field based on vegetation and topography," *Earth Surface Processes and Landforms*, vol. 33, no. 10, pp. 1520–1541, Dec. 2007, https://doi.org/10.1002/esp.1621.

[41] W. Luo, Z. Dong, G. Qian, and J. Lu, "Wind tunnel simulation of the three-dimensional airflow patterns behind cuboid obstacles at different angles of wind incidence, and their significance for the formation of sand shadows," *Geomorphology*, vol. 139–140, pp. 258–270, Feb. 2012, https://doi.org/10.1016/j.geomorph.2011.10.027.

[42] W. Luo, Z. Dong, G. Qian, and J. Lu, "Near-wake flow patterns in the lee of adjacent obstacles and their implications for the formation of sand drifts: A wind tunnel simulation of the effects of gap spacing," *Geomorphology*, vol. 213, pp. 190–200, May 2014, https://doi.org/10.1016/j.geomorph.2014.01.008.

[43] W. Luo, J. Lu, G. Qian, and Z. Dong, "Influence of the gap ratio on variations in the surface shear stress and on sand accumulation in the lee of two side-by-side obstacles," *Environmental Earth Sciences*, vol. 75, no. 9, Apr. 2016, Art. no. 766, https://doi.org/10.1007/s12665-016-5588-3.

[44] M. Mainguet and L. Canon, "Vents et paléo vents du Sahara. Tentative d'approche paléoclimatique," *Revue de géologie dynamique et de géographie physique*, vol. 18, no. 2–3, pp. 241–250, 1976.

[45] M. T. Benazzouz, "Morphogenèse éolienne et principes de fixation des dunes mobiles : élaboration d'un plans d'action dans le Bassin du Hodna et des Ziban (Algérie)," presented at the Séminaire international sur les techniques de fixation des dunes, Taghit, Algeria, Nov. 2001.

[46] N.O.A.A., "National Centers for Environmental Information (NCEI) formerly known as National Climatic Data Center (NCDC) / NCEI offers access to the most significant archives of oceanic, atmospheric, geophysical and coastal data." https://www.ncdc.noaa.gov/.

[47] USGS servey, "EarthExplorer." https://earthexplorer.usgs.gov/.

[48] J. Takaku, T. Tadono, and K. Tsutsui, "ALOS Global Digital Surface Model (AW3D30)." JAXA Earth Observation Research Center, Jan. 2021, https://doi.org/10.5069/G94M92HB.

[49] H. Xianguang, J. Bergström, and Y. Jie, "Distinguishing anomalocaridids from arthropods and priapulids," *Geological Journal*, vol. 41, no. 3–4, pp. 259–269, Sep. 2006, https://doi.org/10.1002/gj.1050.

[50] Z. An, K. Zhang, L. Tan, Q. Niu, and T. Wang, "Mechanisms Responsible for Sand Hazards Along Desert Highways and Their Control: A Case Study of the Wuhai–Maqin Highway in the Tengger Desert, Northwest China," *Frontiers in Environmental Science*, vol. 10, May 2022, https://doi.org/10.3389/fenvs.2022.878778.

[51] Y. Callot, "Géomorphologie et paléoenvironnements de l'atlas saharien au grand erg occidental : dynamique éolienne et paléo-lacs holocènes," PhD dissertation, Université Pierre et Marie Curie, Paris, France, 1987.

[52] R. A. Bagnold, "Forme des dunes de sable et régime des vents," *Actions eoliennes*, vol. 35, pp. 23–32, 1953.

[53] O. Antonić and T. Legović, "Estimating the direction of an unknown air pollution source using a digital elevation model and a sample of deposition," *Ecological Modelling*, vol. 124, no. 1, pp. 85–95, Dec. 1999, https://doi.org/10.1016/S0304-3800(99)00149-0.

[54] D. A. Spera, "Characteristics of the Wind," in *Wind turbine technology*, 2nd ed., USA: U.S. Department of Energy, Office of Renewable Technologies, 1994.

[55] S. Xie, X. Zhang, and Y. Pang, "Wind Dynamic Characteristics and Wind Tunnel Simulation of Subgrade Sand Hazard in the Shannan Wide Valley of the Sichuan–Tibet Railway," *International Journal of Environmental Research and Public Health*, vol. 19, no. 14, Art. no. 8341, Jul. 2022, Art. no. 8341, https://doi.org/10.3390/ijerph19148341.

[56] D. L. Elliott and W. R. Barchet, *Wind Energy Resource Atlas: Volume 1 - The Northwest Region*, vol. 1. Richland, WA, USA: Batteile Pacific Northwest Laboratory, 1980.

[57] D. L. Elliott, C. G. Holladay, W. R. Barchet, H. P. Foote, and W. F. Sandusky, *Wind Energy Resource Atlas of the United States*. Richland, WA, USA: Solar Technical Information Program, Solar Energy Research Institute, 1986.

[58] J. F. Manwell, J. G. McGowan, and A. L. Rogers, *Wind Energy Explained: Theory, Design and Application*, 2nd ed. West Sussex, UK: John Wiley & Sons Ltd, 2010.

[59] S. K. Grange, "Averaging wind speeds and directions," University of Auckland, Auckland, New Zealand, Technical report 12, Jun. 2014, https://doi.org/10.13140/RG.2.1.3349.2006.

[60] M. S. Guettouche and M. Guendouz, "Modélisation et évaluation de l'érosion éolienne potentielle des sols cultivables dans le Hodna (Nord-Est algérien)," *Science et changements planétaires/Sécheresse*, vol. 18, no. 4, pp. 254–262, 2007, https://doi.org/10.1684/sec.2007.0097.

[61] J. Tricart, "Review: Aspects des déserts," *Annales de Géographie*, vol. 87, no. 479, pp. 88–94, Jan. 1978.